Thin-film luminescent solar concentrators: A device study towards rational design

Gianmarco Griffini*, Marinella Levi, Stefano Turri

Department of Chemistry, Materials and Chemical Engineering "Giulio Natta", Politecnico di Milano, Piazza Leonardo da Vinci 32, 20133 Milano, Italy

Received 7 March 2014
Accepted 2 January 2015
Available online 24 January 2015

1. Introduction

In the quest for environmentally sustainable and renewable energy sources, the use of solar power represents one of the most interesting strategies to face the world's steady increase in energy demand and consumption and the simultaneous need of reducing the environmental impact of fossil-fuel based energy sources [1]. Photovoltaic (PV) systems represent one of the most promising approaches to harness such enormous amount of energy from the sun and make it readily available for consumption *via* the direct conversion of sunlight into electricity. Although significant improvements have been made in the past decades in the manufacture of increasingly more efficient PV cells, several weak aspects of this technology are yet to be overcome, among which the cost of PV cells and modules still represent a burden for their widespread diffusion [2]. One possible way to reduce manufacturing and installation costs of traditional PVs and simultaneously achieve improved light management in the system is to make use of luminescent solar concentrators (LSCs) [3–6]. The basic idea behind the LSC concept is the replacement of a large expensive PV cell area with an inexpensive polymer-based thin film or plate collector doped with luminescent species, so that a large amount of photons can be harvested and re-emitted by the luminophore and redirected in waveguide mode towards small-area PV cells placed on the edges of the LSC, where the photon-to-electricity conversion may occur [7–9]. Although the efficiency of an LSC is expected to be lower than an equivalent area of conventional silicon (Si)-based PVs due to the narrower spectral response of the luminescent materials used for LSCs compared with Si, the possibility to employ low cost materials for their fabrication may lead to a prospective reduction of the overall costs associated with solar electricity generation [9]. In addition, this technology may also offer some advantages in terms of architectural integration, where its light weight, tunability of color and shape and ability to work well under diffuse light may allow to overcome some of the intrinsic limitations of conventional inorganic-based PV systems [10–13]. Compared to the more conventional bulk-plate configuration, in which a polymeric slab that also acts as the waveguide is lightly doped with the luminescent species, the thin film LSC configuration presents some technological advantages due to the possibility of depositing the more heavily doped thin luminescent film as a conventional

* Corresponding author. Tel.: +39 02 2399 3213.
E-*mail address:* gianmarco.griffini@polimi.it (G. Griffini).

coating potentially on any transparent substrate with appropriate optical properties, thus further widening the applicability of this technology [14–16].

Recent research efforts have been largely concentrated on critical aspects related to materials synthesis and development. In particular, in the attempt to achieve optical and device efficiencies suitable for practical applications, different new luminescent systems with high efficiency and improved photostability have been proposed [17–24], with organic dyes being by far the most widely exploited. These studies have led to record power conversion efficiencies in the range 4–7% by coupling LSCs with multiple PV cells of different types [25–27]. In addition, new polymeric or hybrid host matrices have also been proposed with the purpose of improving the optical properties of the polymeric carrier or to prevent device performance deterioration and lifetime decrease [28–32].

Although most of the work on LSC technology has been focused on the identification of the most efficient luminophore/host matrix material combination, device design and optimization also represent key issues to further enhance the optical and power conversion efficiency of LSC systems to enable full exploitation of their potential [33]. In particular, a comprehensive investigation on the effects of device configuration on the performance and on the optical and photophysical response of planar thin-film LSC devices is still lacking, although it would be highly desirable to allow for rational thin-film LSC design.

In this work, the photophysical and PV properties of planar thin-film LSC systems have been investigated by correlating their behavior with different device parameters, such as luminophore concentration, LSC film thickness and geometric gain. In addition, the efficiency gain attainable with the use of a white distributed back reflector (WDBR) has also been examined and correlated with WDBR composition and thickness. The ultimate aim of this study is to achieve a greater understanding of the relationships between key LSC device parameters and the photophysical and PV behavior of planar thin film LSC systems, and to provide useful guidelines for a rational approach to thin-film LSC device optimization.

2. Experimental

2.1. Materials

All materials employed in this study are of commercial source and were used as received. A perylene-based fluorescent dye (Lumogen F Red 305, BASF) was used as the fluorescent doping species in the systems investigated in this work. Its molecular structure and its absorption and emission spectra are presented in the Supporting information. Poly (methyl methacrylate) – PMMA (Perspex XT, Lucite) was used as the polymeric carrier for the fabrication of the thin-film LSCs. Titanium dioxide TiO_2 (Ti-Pure R706, Du Pont) was used as the white pigment for the preparation of WDBRs. Chloroform (Sigma Aldrich) was used as solvent in the preparation of all systems.

2.2. Instrumentation

UV–vis, and fluorescence spectroscopy were performed on solid state samples deposited onto glass/quartz substrates by spin-coating (WS-400B-NPP Spin-Processor, Laurell Technologies Corp.) at 1200 RPM for 40 s in air. The coating thickness and root-mean-square surface roughness R_{RMS} were measured by optical profilometry (Microfocus, UBM). UV–vis absorption spectra were recorded in air at room temperature in transmission mode by means of a Jasco V-570 UV-VIS-NIR Spectrophotometer. Fluorescence emission spectra were recorded in air at room temperature on a Jasco FP-6600 Spectrofluorometer. External quantum efficiency measurements were performed on an Oriel QE-PV-SI apparatus equipped with a lock-in amplifier. Gloss measurements were performed on a MultiGloss 268 by Konica Minolta. The illuminated LSC devices were characterized by recording current–voltage (I–V) curves by means of a Keithley 2612 source-measure unit under AM 1.5G solar illumination at 1000 W m^{-2} (1 sun) (Abet Technologies 150 W solar simulator), calibrated with a NREL certified reference cell (PV Measurements). I–V testing was carried-out in air by performing scans between −0.2 V and 0.6 V with 10 mV steps on the illuminated LSC device and by recording the current response. The solar simulator power output was monitored by means of a power-meter with thermopile sensor (Ophir).

2.3. Device fabrication

All LSC devices were fabricated on glass substrates (Thermo Scientific). Solid PMMA was dissolved in chloroform under magnetic stirring, in the presence of the organic luminescent dye. The dye-doped PMMA solutions were then spin-cast onto the glass substrate in air (1200 RPM, 40 s) and allowed to dry out in air after the spin-casting process prior to further processing. In order to investigate the effects of dye concentration on the emission properties of LSC films and on device behavior, the amount of organic dye was varied between 0.01 wt. % and 10 wt. %. Similarly, the concentration of PMMA in chloroform was varied between 5 wt. % and 20 wt. % to allow for different LSC film thicknesses to be explored. The final LSC thickness was found to be in the 2 μm–13 μm. The so-formed LSC films were coupled to a mc-Si PV cell (SLSD-71N400 – active area 45.2 mm^2, average power conversion efficiency of 9.5%, by Silonex Inc.) so that one edge of the glass substrate was connected to the photoactive area of the PV cell (the external quantum efficiency of the mc-Si PV cells used in this work is shown in the Supporting information). Bonding was performed by means of a hotmelt thermosoftening polyurethane adhesive (Krystalflex PE399, by Huntsman Polyurethanes) 0.5 mm thick that was placed on the active face of the PV cell after positioning the PV cell face-up on a 140 °C hot-plate. Once softening of the polyurethane film was achieved (approximately 2 min at 140 °C), one edge of the LSC glass substrate was pressed onto the adhesive film for about 30 s to ensure a good optical contact with the solar cell. The LSC system was then allowed to cool down to room temperature so that hardening of the polyurethane could be achieved. This ensured firm bonding between the solar cell and the LSC and good handling resistance. A schematization of the LSC device structure employed in this study is presented in the Supporting Information. For the preparation of the white back-reflectors, the desired amount of TiO_2 (concentrations between 1 wt. % and 20 wt. % with respect to PMMA were investigated) was added to a chloroform solution of PMMA (5–15 wt. %) and allowed to magnetically stir for two hours. The solution was then placed in an ultrasonic bath for one hour to allow good dispersion of the TiO_2 powder and thus minimize the formation of large TiO_2 aggregates. Finally, the TiO_2-doped PMMA solution was deposited onto a 100 mm × 100 mm glass substrate *via* spin-coating (600 RPM, 40 s) and dried in air. During testing, the back reflector was placed under the LSC device with a 3 mm air gap.

3. Results and discussion

The PV response of LSC systems is commonly considered as the representative parameter for evaluating their device performance. In this work, the PV behavior of LSC devices under standard

illumination conditions was estimated in terms of their optical efficiency η_{opt}, defined as [27]:

$$\eta_{opt} = \frac{\eta_{LSC}}{\eta_{PV}} \quad (1)$$

where η_{PV} is the power conversion efficiency of the PV cell under front-face direct illumination and η_{LSC} is the power conversion efficiency of the LSC device based on the total LSC surface area, namely:

$$\eta_{LSC} = FF\frac{(I_{SC}/A^{(LSC)})V_{OC}}{P_{IN}} \quad (2)$$

with FF [−], I_{SC} [mA], V_{OC} [V], $A^{(LSC)}$ [cm^2] being the fill factor, the short-circuit current, the open-circuit voltage and the front area of the LSC device, respectively and P_{IN} the incident solar power density [mW cm^{-2}].

The PV response of LSC devices as a function of the concentration of luminescent species is reported in Fig. 1. As shown in the plot, by progressively increasing the concentration of luminescent species in the LSC thin film, η_{opt} is found to increase up to a maximum for a dye concentration of 5% (η_{opt} = 4.8%). By further increasing dye concentration, a drop in η_{opt} is observed, leading to η_{opt} values as low as 4% for high dye concentration (10%).

These trends may be explained by considering two counteracting effects occurring in the LSC system at increasing dye concentration. On the one side, an increasing amount of dye molecules in the LSC thin film results in a progressively higher fraction of incident photons to be absorbed (increased optical density), re-emitted (by fluorescence) and made available to the PV cell for light-to-electricity conversion. This results in increased LSC device performance. On the other side, a higher concentration of dye molecules may increase the probability of re-absorption events to occur in the LSC thin film before fluorescence photons can reach the PV cell, due to the partial overlap between absorption and emission spectra of the dye and because of the decreasing dye-to-dye intermolecular distance with increasing dye concentration. Additionally, an increased concentration of dye molecules may lead to the formation of dimers and aggregates, resulting in decreased fluorescence [34,35]. Both these phenomena may be responsible for the decrease in η_{opt} observed at high dye concentrations.

In the attempt to correlate the PV behavior of the LSC devices with their photophysical properties, UV−vis absorption and fluorescence emission spectra were collected at increasing dye concentration and the results are presented in Fig. 2. As shown in the plots, the absorption intensity is found to progressively increase with dye concentration, as expected (Fig. 2a). As opposed to this, the fluorescence emission intensity reaches a maximum for 5% dye concentration, above which a sharp decrease is observed (for 10% dye concentration) (Fig. 2b).

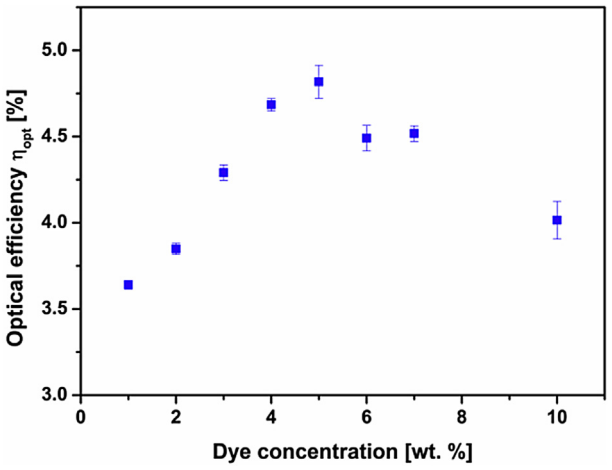

Fig. 1. Optical efficiency η_{opt} of LSC devices as a function of dye concentration.

From the plot of fluorescence emission intensity vs. absorption intensity (Fig. 3) it can be noted that while a steady increase of the emission intensity with absorbance is observed for dye concentrations up to 5%, when dye concentration is further increased the emission intensity undergoes a sharp decrease in spite of the significant increase in absorption intensity. This behavior indicates that for highly concentrated LSC films (>5% dye concentration) a portion of the absorbed photons is lost *via* dissipative processes.

It was recently shown on similar systems [29,36] that the formation of aggregates at high dye concentrations may lead to fluorescence quenching. In addition, in some systems such aggregates were shown to promote the formation of low-energy electronic states (such as excimers) that may act as trapping sites for emitted photons, thus leading to a decrease in photoluminescence quantum yield [37]. Along these lines, also in the present work formation of dye aggregates may be partly responsible for the observed decrease of fluorescence intensity for dye concentrations above a threshold value of 5%, due to the relatively high dye concentrations employed here. Another parallel effect that may lead to a decreased luminescence at increasing dye concentration may be related to the progressively higher re-absorption losses occurring in the LSC thin film. For increasing dye concentrations, the optical density of the LSC film increases and this may yield a higher probability for an emitted photon to be re-absorbed by another adjacent dye molecule, thus preventing the fluorescence from leaving the LSC plate. In this work, this effect appears relevant above a threshold dye concentration of 5%. It is interesting to note that the trends observed on fluorescence emission intensity discussed so far well correlate with the PV response of LSC devices as presented in Fig. 1 above, where a maximum value of η_{opt} was found for the same threshold dye concentration.

In addition to a change in the peak emission intensity, a progressive bathochromic shift of the fluorescence emission peak is also observed as the dye concentration is increased (see inset to Fig. 2b). In particular, a 17 nm red-shift of the emission spectrum is observed when the concentration of the dye is increased from 0.01% to 10%. Since no spectral shifts were found in the UV−vis absorption spectra at varying dye concentration (Fig. 2a), the red-shift observed in the fluorescence spectra results in an increased Stokes shift of the fluorophore with increasing dye concentrations (from 23 nm to 40 nm for dye concentration of 0.01% and 10%, respectively). Two concurrent effects may be responsible for the observed spectral shifts. An increased re-absorption due to higher dye concentration (shorter dye-to-dye distance) results in the re-emission of (second generation) photons with progressively longer wavelength. However, at higher dye concentrations the formation of dye aggregates also becomes increasingly more relevant. Such aggregates were shown to exhibit red-shifted absorption and emission spectra as compared with single dye molecules [34]. Therefore, long wavelength second generation photons may induce excitation of such aggregates, whose fluorescence leads to progressively red-shifted emission spectra. Since formation of dye aggregates is closely related to the concentration of the dye molecules in the LSC thin film, this phenomenon appears progressively more relevant as the dye concentration is increased.

In addition to varying the amount of fluorescent dye, the effect of LSC film thickness on device performance was also investigated. To this end, the concentration of the starting PMMA solution in chloroform to be deposited on the glass waveguide was

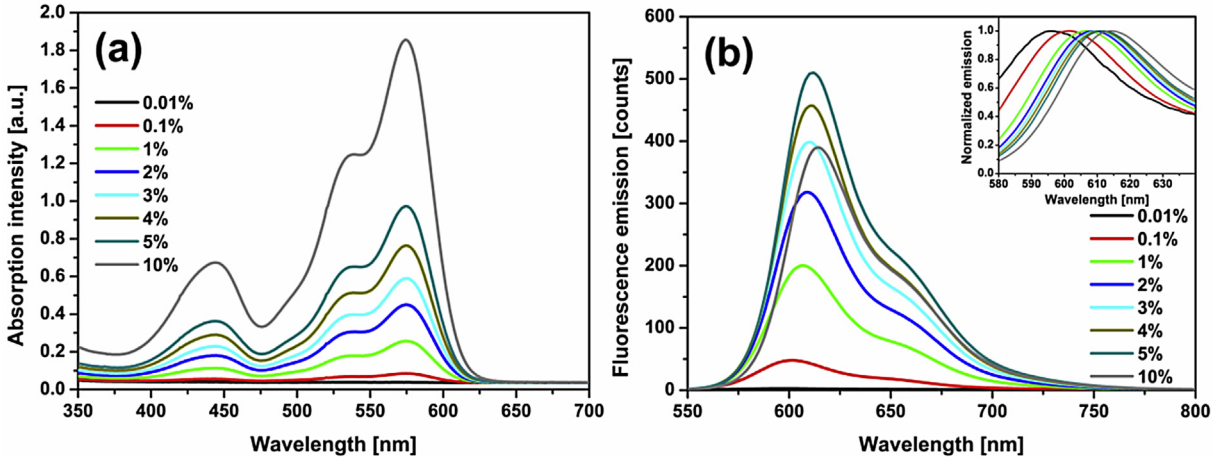

Fig. 2. (a) UV–vis absorption and (b) fluorescence emission spectra LSC thin films at increasing dye concentration.

progressively increased at constant dye concentration (5 wt. %) so as to achieve LSC film thicknesses in the range 2 μm–13 μm. The corresponding LSC devices were then fabricated and tested, and their η_{opt} is presented in Fig. 4a.

By progressively increasing the thickness of the LSC film, the PV performance is found to increase until a plateau value of $\eta_{opt} \approx 5.2\%$ is reached for a thickness above 8 μm. In order to better clarify this behavior, UV–vis and fluorescence emission spectra were collected for LSCs with increasing film thickness (Supporting Information). As expected, a higher film thickness leads to a more intense UV–vis absorption. However, a different trend is found on the emission properties. As shown in Fig. 4b, where the peak fluorescence emission intensity is plotted as a function of the peak absorption intensity for systems at different thicknesses, the emission intensity is found to increase linearly with the absorption intensity for film thicknesses up to 5 μm, indicating a negligible effect of dissipation phenomena. However, when the thickness is further increased a deviation from linearity is observed. In particular, the increase of absorption intensity is higher than the corresponding increase in emission intensity, thus indicating that dissipative phenomena take place. As also found in LSC films with increasing dye concentration, this effect may be due to the occurrence of re-absorption events that may cause a decrease of the number of re-emitted photons. As a result, a progressively higher loss of fluorescence (increasing dissipation) may be observed as the film thickness is increased. This trend well correlates with the results obtained from the PV characterization of LSC devices (Fig. 4a).

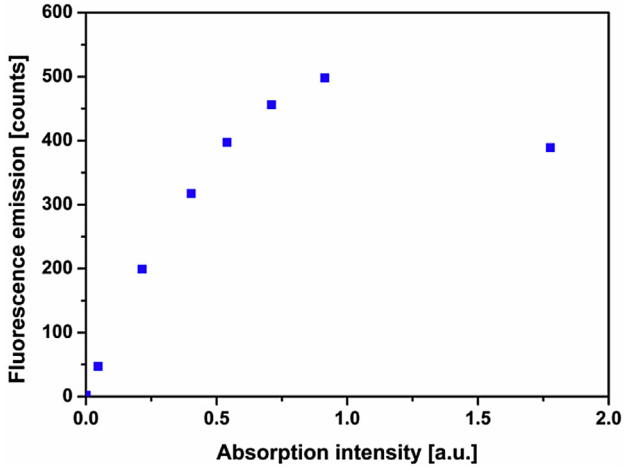

Fig. 3. Fluorescence peak emission intensity vs. UV–vis peak absorption intensity (absorbance) of LSC thin films with increasing dye concentration.

To further explore the effect of device parameters on PV performance, LSCs with different geometric gains G ($= A_{LSC}/A_{PV}$) were fabricated and tested. In particular, G values between 7 and 42 were considered by progressively increasing the length of the LSC at constant width (25 mm), and by maintaining constant dye concentration (5 wt. %) and constant LSC film thickness (9 μm) for all devices.

As shown in Fig. 5a, a sharp decrease of optical efficiency of LSC devices at increasing G is observed for G values lower than 25, which appears to level off for higher G values. This behavior may be explained by considering the balance between two distinct and counteracting effects. For large G values, a higher number of luminescent molecules are available for photon absorption and re-emission compared to low-G devices because of the increased active area of the LSC. This results in a higher number of absorbed and re-emitted photons theoretically available for the photon-to-current conversion by the PV cell. However a larger area LSC device also implies that re-emitted photons have to travel on average a longer distance before reaching the PV cell on the LSC edge. This increased photon path length may result in a higher probability of fluorescence re-absorption by other adjacent dye molecules or in a higher probability of photon loss *via* the escape cone. As a result, higher G values lead to lower LSC performance, as also evident from external quantum efficiency measurements carried out on the same systems (Supporting information). It is worth noticing that, by further increasing G, the negative contribution to η_{opt} given by re-absorption and escape cone losses seems to be well compensated by the increased amount of re-emitted photons available because of the increased surface area of the LSC device, so that a plateau value for η_{opt} seems to be reached. This behavior indicates that LSC devices perform best for very high G values. Accordingly, the concentration factor C ($= G\ \eta_{opt}$) is found to progressively increase with G (Fig. 5b). These results are in good agreement with previous reports on similar systems [26,38].

In order to achieve optimal LSC device operation, a distributed back reflector is often employed in conjunction with the luminescent film with the function of redirecting back towards the waveguide the photons transmitted through or escaped from the back of the luminescent film/waveguide system. As a result, an improvement of LSC performance can be achieved because a higher number of photons is able to travel in the waveguide by total internal

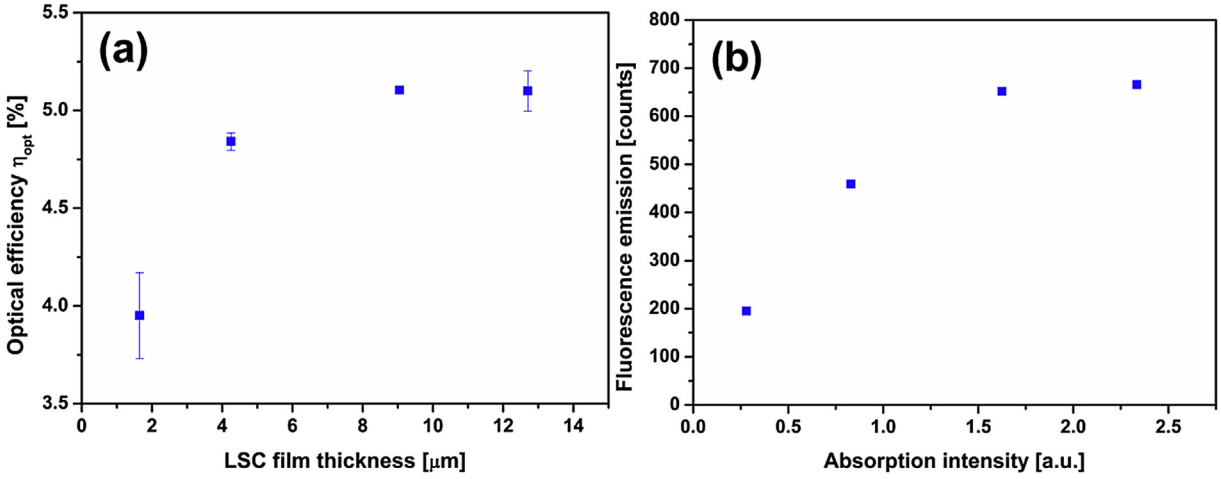

Fig. 4. (a) Optical efficiency η_{opt} of LSC devices as a function of LSC film thickness and (b) fluorescence peak emission intensity vs. UV–vis peak absorption intensity of LSC thin films with increasing film thickness.

reflection and made available for the PV cell. In this work, a dispersion of TiO_2 nanoparticles in a polymeric binder (PMMA) was used as the precursor for the spin-coating deposition of the WDBR film. In the attempt to correlate the effects of WDBR composition with the PV performance of the LSC devices, TiO_2 concentration (1–10 wt. % on binder) and WDBR film thickness (2–14 μm) were systematically varied, while all other LSC device parameters were maintained constant (5 wt. % dye concentration, 9 μm LSC thin film thickness, G = 28). To evaluate the improvement in performance attained with the use of a WDBR as compared to an LSC device with no WDBR, the optical efficiency gain $\Delta\eta_{opt}$ was used as the figure-of-merit, defined as:

$$\Delta\eta_{opt} = \frac{\eta_{opt}^{WDBR} - \eta_{opt}^{0}}{\eta_{opt}^{0}} \quad (3)$$

where η_{opt}^{WDBR} and η_{opt}^{0} are the optical efficiencies of the LSC system with and without WDBR, respectively. The reference η_{opt}^{0} was calculated by performing tests on the LSC device placed on a black support.

As shown in Fig. 6a, where $\Delta\eta_{opt}$ as a function of TiO_2 concentration is presented, an increase in TiO_2 concentration yields a progressively higher $\Delta\eta_{opt}$ irrespective of the WDBR film thickness considered. In addition, thicker WDBR films appear to yield better PV performance at constant TiO_2 concentrations, especially for high TiO_2 loading. These trends may be explained by considering that for higher concentrations of TiO_2 the hiding power of the WDBR film becomes more intense, thus leading to a more efficient scattering process of photons transmitted through the LSC film that are sent back to the transparent waveguide and made available to the dye molecules in the LSC thin film for a new absorption/emission event. Similar trends were also observed on I_{SC} at increasing TiO_2 concentration (Supporting Information), as a consequence of the larger amount of photons resulting from the scattering process that can be re-absorbed by dye molecules and can in turn be re-emitted and made available for the waveguiding process.

In the attempt to correlate the trends observed in Fig. 6a on LSC devices with the morphology of the WDBR films, roughness measurements were carried out on all WDBR films investigated, and the results are presented in Fig. 6b. As shown in the plot, by increasing TiO_2 content for a fixed film thickness, an increase of R_{RMS} is observed. This may be due to an increasing amount of TiO_2 nanoparticles in the dispersion lying on the surface of the WDBR film and thus contributing to the increase of surface roughness. In addition, an increase of R_{RMS} is found as the WDBR film thickness is

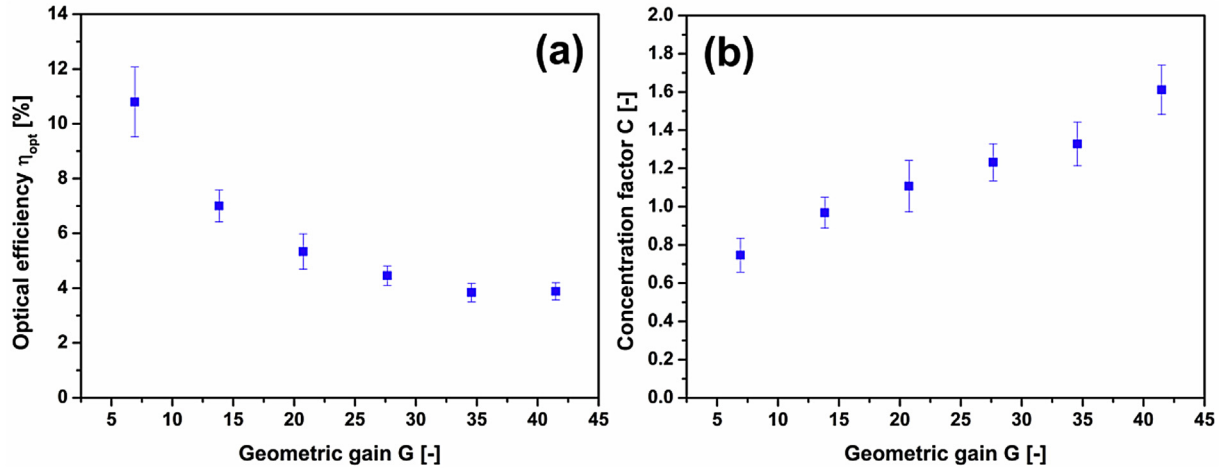

Fig. 5. (a) Optical efficiency η_{opt} and (b) concentration factor C of LSC devices as a function of geometric gain G.

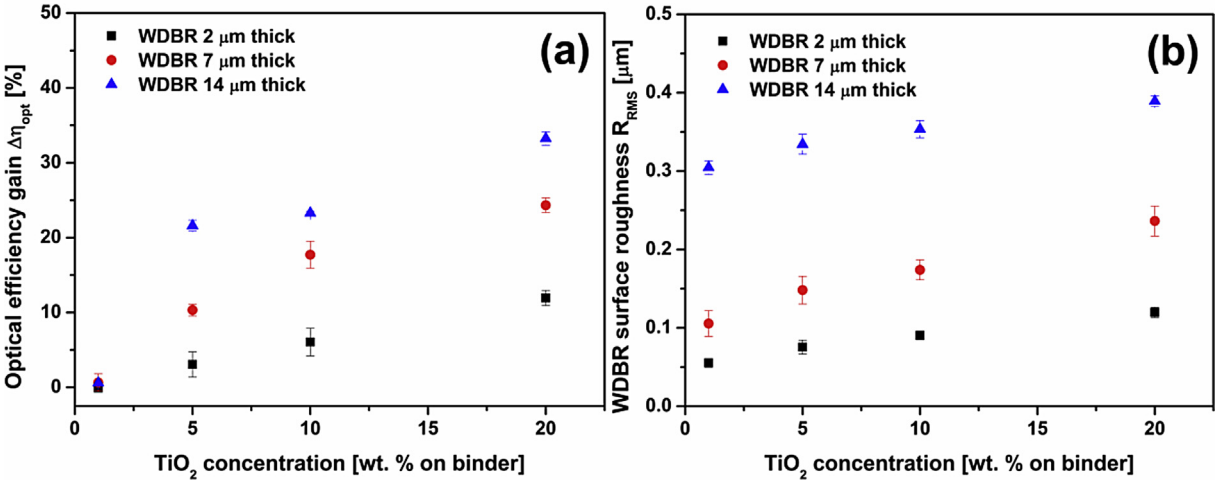

Fig. 6. (a) Optical efficiency gain $\Delta\eta_{opt}$ of LSC devices and (b) white distributed back reflector (WDBR) surface roughness R_{RMS} for increasing TiO_2 concentration and WDBR thickness.

increased. This behavior may be ascribed to the increasingly higher viscosities of the TiO_2/PMMA dispersions used for the spin-coating deposition of high thickness WDBR films (increased binder concentration at constant spin-coating speed) that yield progressively rougher and inhomogeneous WDBR thin films.

The effect of WDBR surface roughness on the PV response of the LSC devices may be related to the changes of the specular reflectivity of the WDBR film with TiO_2 concentration. To better clarify this aspect, surface gloss measurements were performed on all WDBR systems investigated in this work. Gloss measurements represent a fast and convenient way to estimate the reflective properties of a surface [39]. In particular, surface gloss can be generally associated with the ability of a surface to reflect incident light in a preferential (specular) direction [40,41]. As shown in Fig. 7, where the gloss unit G.U. and R_{RMS} are plotted as a function of TiO_2 concentration for 2 μm thick WDBR films, G.U. appears to decrease as TiO_2 concentration is increased, as opposed to what found for R_{RMS}. This trend indicates that the ability of the WDBR to reflect light specularly decreases as TiO_2 (R_{RMS}) is increased. In fact, a higher specular reflectivity is commonly obtained in highly polished, very low roughness surfaces. As a result, when a high roughness-low gloss WDBR film is employed, photons transmitted through the LSC can be reflected back and scattered to the fluorescent film isotropically, thus leading to a higher probability for such reflected photons to be conveyed to the PV cell through the transparent waveguide. This explains the increase of $\Delta\eta_{opt}$ observed in LSC systems with WDBR films with increasing TiO_2 concentration. The same trends were observed also on thicker WDBR films, thus indicating that such behavior appears to be independent of WDBR film thickness (Supporting Information).

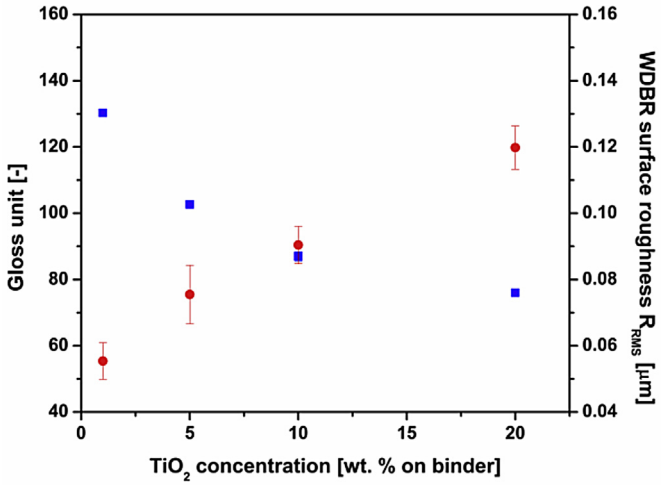

Fig. 7. Gloss unit and R_{RMS} surface roughness of 2 μm thick WDBR films as a function of TiO_2 concentration.

4. Conclusions

In this work, the effect of different device parameters on the photophysical and PV behavior of thin film LSC systems was investigated. In particular, luminescent dye concentration, luminescent film thickness, geometric gain and composition of WDBR film were systematically varied and their influence on LSC thin film properties and device performance was examined. It was shown that by varying dye concentration, η_{opt} of LSC devices was found to reach a maximum for a dye concentration of 5 wt.%, as also inferred from spectroscopic characterization of the LSC thin films. In particular, it was shown that higher dye concentrations led to an increased probability of dye aggregation and re-absorption losses that yielded a drop in device performance, while for lower dye concentrations the lower optical density of the luminescent film yielded non-optimal device performance. Furthermore, a plateau value of η_{opt} was attained by progressively increasing LSC film thickness, due to the balance between the increase of optical density of the LSC film (higher photon absorption) and the progressive increase of losses due to re-absorption of emitted photons by adjacent dye molecules, which become more relevant as the LSC film thickens. In addition, a sharp decrease of η_{opt} was found in LSC devices at increasing geometric gain, due to the increased path length emitted photons have to travel within the waveguide before reaching the PV cell, resulting in a higher probability of fluorescence re-absorption by other adjacent dye molecules or in a higher probability of photon loss *via* the escape cone. However, for high values of G (G > 30) the negative contribution to η_{opt} given by re-absorption and escape cone losses was found to be compensated by the increased amount of absorbed and emitted photons resulting from the larger surface area of the LSC device. This behavior indicates that LSC devices perform best for very high G values.

Finally, by employing a WDBR as back scatterer of photons transmitted through or leaving the LSC film, η_{opt} was shown to increase, with a higher PV performance improvement found on LSCs coupled to WDBR films with high surface roughness. This behavior was explained by the decrease of specular reflectivity of the WDBR film, which was found to decrease at increasing surface roughness, thus leading to improved PV performance.

In conclusion, the results of this study provide a greater understanding of the influence of device parameters on the behavior of thin-film LSC systems, and give useful guidelines for the device optimization and rational design of thin-film LSC devices.

Acknowledgments

The authors gratefully acknowledge Dr. Luigi Brambilla, Prof. Mirella Del Zoppo and Prof. Chiara Castiglioni for helpful discussions.

Appendix A. Supplementary data

Supplementary data related to this article can be found on line.

References

[1] Smith GB, Granqvist C-GS. Green Nanotechnology: solutions for Sustainability and Energy in the Built Environment. CRC Press; 2010.
[2] Green MA. Third generation photovoltaics: ultra-high conversion efficiency at low cost. Prog Photovoltaics 2001;9:123–35.
[3] Farrell DJ, Yoshida M. Operating regimes for second generation luminescent solar concentrators. Prog Photovoltaics 2012;20:93–9.
[4] Currie MJ, Mapel JK, Heidel TD, Goffri S, Baldo MA. High-efficiency organic solar concentrators for photovoltaics. Science 2008;321:226–8.
[5] Scudo PF, Abbondanza L, Fusco R, Caccianotti L. Spectral converters and luminescent solar concentrators. Sol Energy Mater Sol Cells 2010;94:1241–6.
[6] Yoon J, Li LF, Semichaevsky AV, Ryu JH, Johnson HT, Nuzzo RG, et al. Flexible concentrator photovoltaics based on microscale silicon solar cells embedded in luminescent waveguides. Nat Commun 2011;2.
[7] Smestad G, Ries H, Winston R, Yablonovitch E. The thermodynamic limits of light concentrators. Sol Energy Mater 1990;21:99–111.
[8] Rau U, Einsele F, Glaeser GC. Efficiency limits of photovoltaic fluorescent collectors. Appl Phys Lett 2005;87.
[9] Debije MG, Verbunt PPC. Thirty years of luminescent solar concentrator research: solar energy for the built environment. Adv Energy Mater 2012;2:12–35.
[10] Kocher-Oberlehner G, Bardosova M, Pemble M, Richards BS. Planar photonic solar concentrators for building-integrated photovoltaics. Sol Energy Mater Sol Cells 2012;104:53–7.
[11] Zhao Y, Lunt RR. Transparent luminescent solar concentrators for large-area solar windows enabled by massive Stokes-Shift nanocluster phosphors. Adv Energy Mater 2013;3:1143–8.
[12] Wiegman JWE, van der Kolk E. Building integrated thin film luminescent solar concentrators: detailed efficiency characterization and light transport modelling. Sol Energy Mater Sol Cells 2012;103:41–7.
[13] Corrado C, Leow SW, Osborn M, Chan E, Balaban B, Carter SA. Optimization of gain and energy conversion efficiency using front-facing photovoltaic cell luminescent solar concentrator design. Sol Energy Mater Sol Cells 2013;111: 74–81.
[14] Bose R, Farrell DJ, Chatten AJ, Pravettoni M, Buchtemann A, Barnham KWJ. Novel configurations of luminescent solar concentrators. In: Proc. of 22nd European photovoltaic solar Energy Conference (22nd EUPVSEC), Milan, Italy; 2007. p. 210–4.
[15] Reisfeld R, Shamrakov D, Jorgensen C. Photostable solar concentrators based on fluorescent glass-films. Sol Energy Mater Sol Cells 1994;33:417–27.
[16] El Bashir SM, Barakat FM, AlSalhi MS. Metal-enhanced fluorescence of mixed coumarin dyes by silver and gold nanoparticles: towards plasmonic thin-film luminescent solar concentrator. J Lumin 2013;143:43–9.
[17] Seybold G, Wagenblast G. New perylene and violanthrone dyestuffs for fluorescent collectors. Dyes Pigm 1989;11:303–17.
[18] Moudam O, Rowan BC, Alamiry M, Richardson P, Richards BS, Jones AC, et al. Europium complexes with high total photoluminescence quantum yields in solution and in PMMA. Chem Commun 2009:6649–51.
[19] Bozdemir OA, Erbas-Cakmak S, Ekiz OO, Dana A, Akkaya EU. Towards unimolecular luminescent solar concentrators: bodipy-based dendritic energy-transfer cascade with panchromatic absorption and monochromatized emission. Angew Chem Int Ed 2011;50:10907–12.
[20] Bomm J, Buchtemann A, Chatten AJ, Bose R, Farrell DJ, Chan NLA, et al. Fabrication and full characterization of state-of-the-art quantum dot luminescent solar concentrators. Sol Energy Mater Sol Cells 2011;95:2087–94.
[21] El Bashir SM. Photophysical properties of fluorescent PMMA/SiO_2 nanohybrids for solar energy applications. J Lumin 2012;132:1786–91.
[22] Griffini G, Brambilla L, Levi M, Del Zoppo M, Turri S. Photo-degradation of a perylene-based organic luminescent solar concentrator: molecular aspects and device implications. Sol Energy Mater Sol Cells 2013;111:41–8.
[23] El Bashir SM, Barakat FM, AlSalhi MS. Double layered plasmonic thin-film luminescent solar concentrators based on polycarbonate supports. Renew Energy 2014;63:642–9.
[24] Griffini G, Brambilla L, Levi M, Castiglioni C, Del Zoppo M, Turri S. Anthracene/tetracene cocrystals as novel fluorophores in thin-film luminescent solar concentrators. RSC Adv 2014;4:9893–7.
[25] Slooff LH, Bende EE, Burgers AR, Budel T, Pravettoni M, Kenny RP, et al. A luminescent solar concentrator with 7.1% power conversion efficiency. Phys Status Solidi RRL 2008;2:257–9.
[26] Goldschmidt JC, Peters M, Bosch A, Helmers H, Dimroth F, Glunz SW, et al. Increasing the efficiency of fluorescent concentrator systems. Sol Energy Mater Sol Cells 2009;93:176–82.
[27] Desmet L, Ras AJM, de Boer DKG, Debije MG. Monocrystalline silicon photovoltaic luminescent solar concentrator with 4.2% power conversion efficiency. Opt Lett 2012;37:3087–9.
[28] Fattori V, Melucci M, Ferrante L, Zambianchi M, Manet I, Oberhauser W, et al. Poly(lactic acid) as a transparent matrix for luminescent solar concentrators: a renewable material for a renewable energy technology. Energy Environ Sci 2011;4:2849–53.
[29] Buffa M, Carturan S, Debije MG, Quaranta A, Maggioni G. Dye-doped polysiloxane rubbers for luminescent solar concentrator systems. Sol Energy Mater Sol Cells 2012;103:114–8.
[30] Lim YS, Lo CK, Teh GB. Unsaturated polyester resin blended with MMA as potential host matrix for luminescent solar concentrator. Renew Energy 2012;45:156–62.
[31] Griffini G, Levi M, Turri S. Novel crosslinked host matrices based on fluorinated polymers for long-term durability in thin-film luminescent solar concentrators. Sol Energy Mater Sol Cells 2013;118:36–42.
[32] Griffini G, Levi M, Turri S. Novel high-durability luminescent solar concentrators based on fluoropolymer coatings. Prog Org Coat 2014;77: 528–36.
[33] Hernandez-Noyola H, Potterveld DH, Holt RJ, Darling SB. Optimizing luminescent solar concentrator design. Energy Environ Sci 2012;5: 5798–802.
[34] Al Kaysi RO, Ahn TS, Muller AM, Bardeen CJ. The photophysical properties of chromophores at high (100 mM and above) concentrations in polymers and as neat solids. Phys Chem Chem Phys 2006;8:3453–9.
[35] Colby KA, Burdett JJ, Frisbee RF, Zhu L, Dillon RJ, Bardeen CJ. Electronic energy migration on different time scales: concentration dependence of the time-resolved anisotropy and FLUORESCENCE quenching of lumogen red in poly(methyl methacrylate). J Phys Chem A 2010;114:3471–82.
[36] Haines C, Chen M, Ghiggino KP. The effect of perylene diimide aggregation on the light collection efficiency of luminescent concentrators. Sol Energy Mater Sol Cells 2012;105:287–92.
[37] Yoo H, Yang J, Yousef A, Wasielewski MR, Kim D. Excimer formation dynamics of intramolecular pi-stacked perylenediimides probed by single-molecule fluorescence spectroscopy. J Am Chem Soc 2010;132:3939–44.
[38] Kim JM, Dutta PS. Optical efficiency-concentration ratio trade-off for a flat panel photovoltaic system with diffuser type concentrator. Sol Energy Mater Sol Cells 2012;103:35–40.
[39] Nadal ME, Thompson EA. NIST reference goniophotometer for specular gloss measurements. J Coat Technol 2001;73:73–80.
[40] Arney JS, Ye L, Banach S. Interpretation of gloss meter measurements. J Imaging Sci Technol 2006;50:567–71.
[41] Becker ME. Evaluation and characterization of display reflectance. Displays 1998;19:35–54.